ORGANOMETALLICS
Article
Cite This: Organometallics XXXX, XXX, XXX−XXX
pubs.acs.org/Organometallics

Synthesis and Theoretical Investigation of Diphosphastannylenes

Elisabeth Schwarz,* Stefan K. Mueller, Gernot Weinberger, Ana Torvisco, and Michaela Flock*

Institute of Inorganic Chemistry, Graz University of Technology, Stremayrgasse 9/IV, 8010 Graz, Austria

Supporting Information

ABSTRACT: The factors affecting the stabilization of diphosphastannylenes, such as substituent size, steric demand, and type of substituent (aryl, alkyl, silyl) were investigated via a comprehensive DFT and experimental investigation. The influence of various substituents (H, Me, ^{t}Bu, Ph, TMS, Hyp = (Si(SiMe$_3$)$_3$)) on the pyramidalization of the phosphorus centers and cone angle determination of those substituents were carried out. Through these considerations, ligand systems capable of isolating a stable Sn(II) species were determined. Synthetic work led to the isolation of dimeric supermesityl(trimethylsily)phosphanides, 2,4,6-tris(*t*-butyl)phenyl trimethylsilyl lithium phosphanide, 2,4,6-tris(*t*-butyl)phenyl trimethylsilyl potassium phosphanide, and one hypersilylphosphanide [HypP(SiMe$_3$)-K·DME]. In addition to that, a novel monomeric diphosphastannylene [HypP(SiMe$_3$)]$_2$Sn was isolated as well as confirmed by experimental and calculated NMR data and single crystal X-ray analysis.

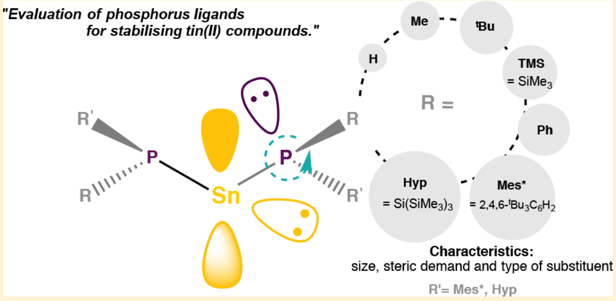

INTRODUCTION

Diphosphatetrylenes, the heavier analogues of the well-known diaminotetrylenes, have gained interest in recent years. The number of publications that examine the analogue cyclic α,α'-nitrogen-stabilized carbenes (NHC, Arduengo carbene[1]) is quite large given that there is just one analogous α,α'-phosphorus-stabilized compound of this type.[2] The acyclic compounds have, because of their high reactivity, substantial possibilities in transition metal catalysis while still showing enough stability for convenient use. Tetrylenes are able to coordinate to transition metals forming homogeneous catalysts, as is impressively shown in the work of Lappert[3] and Veith.[4] In Lappert's investigations with Pd(II) complexes, Sn[N(SiMe$_3$)$_2$] acts as a two-electron σ-donor, which is a successful alternative to the widely used tertiary phosphanes.[5] In diaminotetrylenes, stabilization is provided via interaction of the group 15 element lone pair with the vacant p-orbital on the group 14 element in oxidation state + II (tetrel atom E = C, Si, Ge, Sn, Pb). As a result of the large planarization barrier of the P atom, the effective orbital overlap was discussed as being less beneficial in diphosphatetrylenes,[6] which might be a reason for the small number of compounds in the literature. However, in 1996, Schleyer et al.[7] noted that the inherent p-donor capabilities of phosphorus should be as large or even larger than those of nitrogen. Nevertheless, the difference in the electronegativities (Pauling: N = 3.04, P = 2.19) and the stronger pyramidalization of the phosphorus might counteract the effective orbital overlap with the empty p-orbital of the tetrel atom.

In order to use the tetrylenes for subsequent chemical reactions, the steric shielding should be small enough to allow access to the reactive tetrel center. At the same time, stability needs to be increased by intramolecular donation of electron density into the empty p-orbital on the tetrel (see Figure 1). So the key to success for the stability of diphosphatetrylenes should be the determination of substituents that provide sufficient steric protection, together with decreasing the pyramidalization of the P atom to obtain optimal orbital overlap.

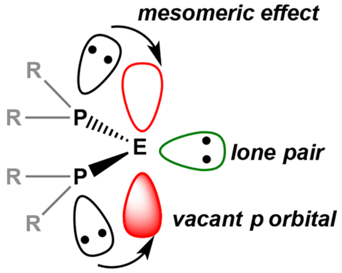

Figure 1. Intramolecular stabilization of diphosphatetrylenes.

In almost all literature known structures, the P atoms are de facto trigonal pyramidal and no typical π-type interactions could be determined. In 1977, the first diphosphatetrylene with the rather small ^{t}Bu substituents, [(^{t}Bu$_2$P)]$_2$Sn$_2$, a dimeric compound,[8] was established via NMR spectroscopy. A few years later, the first monomeric structure (Me$_3$Si)$_2$P$_2$Sn was confirmed by NMR spectroscopy and cryoscopy;[9] red-orange crystals were isolated but decomposed while storing at reduced temperature. Since TMS (=SiMe$_3$) and ^{t}Bu are similar in their steric demand, this indicates that silyl substituents might be more favorable for the stabilization of monomeric diphospha-

Received: April 25, 2018

DOI: 10.1021/acs.organomet.8b00258

tetrylenes compared to alkyl ligands. The first structurally characterized diphosphastannylene was isolated by Driess in 1995,[10] bearing sterically demanding silyl substituents R1R2, on the pyramidal P atom, with R1 = $-Si(2,4,6\text{-}^{i}Pr_3C_6H_2)_2F$ or $-Si(^{t}Bu)(2,4,6\text{-}^{i}Pr_3C_6H_2)F$ and R2 = $-Si(^{t}Bu)(2,4,6\text{-}^{i}Pr_3C_6H_2)F$. A bis(phosphanyl) stannylene was isolated by Westerhausen in 1998. Here, bulky phospholide substituents were used.[11,12] The stabilization via formation of phosphastannenocenes was also mentioned by Brym and Jones.[12]

In 2007, an NMR experiment characterizing monomeric diphosphastannylene, $[Ar^{Mes_2}P(Ph)]_2Sn$ (Ar^{Mes_2} = $C_6H_3-2,6(C_6H_2-2,4,6\text{-}Me_3)$), was reported by Rivard.[13] In 2005 and 2012, comparatively small diphosphatetrylenes, $[(Me_3Si)_2-CH]P(C_6H_4-2\text{-}SMe)_2E$ (E = Ge, Sn) and $[(Ph)(C_6H_3-2,6\text{-}CH_2NMe_2)_2P]_2Sn$ were isolated by Izod[14] and Řezniček.[15] In both cases, additional stabilization of discrete monomers was reached by intramolecular base stabilization via a sulfur or a nitrogen lone pair.

All of the above-mentioned and literature known monomeric diphosphastannylenes feature rather bulky and sterically demanding alkyl, aryl, or silyl substituents[11] on the pyramidal phosphorus atoms. Izod[16] recently also added π-stabilized diphosphatetrylenes to this type of compound, in which one of the phosphorus atoms actually has a planar configuration. These diphosphatetrylenes $(R_2P)_2E$ [E = Ge, Sn; R = Dipp $(2,6\text{-}^{i}Pr_3C_6H_2)$ or Tripp $(2,4,6\text{-}^{i}Pr_3C_6H_2)$][16] show stabilization via pπ−pπ interaction of one trigonal-planar P center. Nevertheless, the substituents used in these compounds are rather bulky groups.

As suggested by Izod, stabilization in diphosphastannylenes could be fortified by a strong P═E multiple bond character.[16] Such a strong intramolecular stabilization could allow the use of smaller substituents for stable tetrylenes. However, what is missing is an understanding in what factors of the ligand, including substituent size, steric demand, and kind of substituent (aryl, alkyl, silyl), affect isolation and stabilization of novel compounds. DFT calculations were used to explore the influence of various substituents (H, Me, ^{i}Pr, ^{t}Bu, Ph, TMS, Hyp = $(Si(SiMe_3)_3)$) on the pyramidalization of the phosphorus center. Cone angle determination of those substituents was carried out. Through these considerations, a ligand system capable of isolating a stable Sn(II) species, was determined.

■ RESULTS AND DISCUSSION

As noted before, Izod[16] recently characterized diphosphastannylenes and -germylenes, bearing rather bulky, aromatic substituents (Dipp, Tripp), where one of the phosphorus centers is planar, and a P═E double bond is formed. Diphosphatetrylenes with smaller silyl substituents on the P atoms, have not been isolated so far, although $SiMe_3$ groups have been used as sterically demanding, stabilizing substituents for several years in group 14 chemistry.[17] In 2006, Hassler et al. reported on several phosphanes and diphosphanes featuring a bulky $-Si(SiMe_3)_3$ group, among others, the simple hypersilylphosphane $[(SiMe_3)_3Si-PH_2]$.[18] The hypersilyl moiety $[(SiMe_3)_3Si-]$ provides great steric protection to neighboring groups while generally not being reactive itself, if not specifically targeted.[18] It was shown that backbone systems featuring a hypersilyl moiety can be functionalized, which might make them ideal precursors for the synthesis of novel α,α'-P-tetrylenes.[18,19] Unlike the ligands of all previously reported monomeric diphosphatetrylenes, these ligands feature neither aromatic nor any additional electron donating moieties.

Computational Approach. For more insight, a DFT investigation of phosphorus ligands with aryl, alkyl, and silyl substituents on the phosphorus atoms was carried out. Owing to the fact that larger substituents are essential for kinetic stabilization, greater focus was placed on 2,4,6-tris(*t*-butyl)-phenyl−PR_2 (Mes*PR_2), which is comparable to the bulky aromatic substituents (Dipp, Tripp) used in literature known diphosphastannylenes, and $HypPR_2$, Hyp = $(Si(SiMe_3)_3)$), as a sterically demanding silyl substituent.

A closer look at the influence of the substituent choice on the planarization using Mes*PR_2 and $HypPR_2$ as root backbones with R = H, Me, ^{t}Bu, TMS, Hyp, and Ph was taken. Comparing the results for both types of phosphanes, the Mes*backbone, seen in Table 1, appears particularly suitable for lowering the pyramidalization of the P atom. Focusing on the ^{t}Bu, TMS, and Hyp substituents, a stronger effect on the pyramidalization for the silyl substituents was observed. Although the TMS group is isomorphic[20] and similar in size to the ^{t}Bu ligand, the bond angle sum (ΣP) increases by 10 degrees going from ^{t}Bu (ΣP = 341.8°) to TMS (ΣP = 351.9°). This indicates that the type (aryl, alkyl, silyl) of substituent is as essential as its size. A second aromatic group, Ph, does not seem to enhance planarity.

Table 1. mPW1PW91/SDD DFT Calculated Geometry Data for Mes*PR_2

R	H	Me	^{t}Bu	TMS	Hyp	Ph
P−C [Å]	1.90	1.89	1.90	1.89	1.90	1.86
P−R [Å]	1.44	1.89	1.96	2.34	2.48	1.87
ΣP [°]	293.4	319.9	341.8	351.9	359.9	326.3

A similar trend is noted for the $HypPR_2$ compounds (see Table 2). However, the bond angle sums around P are approximately 20° smaller for both, ^{t}Bu and TMS. Only Hyp_3P has a rather high bond angle sum with 341.7°. These results suggest a superiority of the Mes*PR_2 substituent for forming E═P double bonds.

Table 2. mPW1PW91/SDD DFT Calculated Geometry Data for $HypPR_2$

R	H	Me	^{t}Bu	TMS	Hyp	Ph
P−Si [Å]	2.36	2.36	2.41	2.36	2.43	2.38
P−R [Å]	1.44	1.90	1.95	2.35	2.49	1.88
ΣP [°]	287.0	303.1	321.5	333.1	341.7	312.1

Calculations of Cone Angles. Steric bulk of ligands is usually determined by Tolman θ or solid cone angles Θ,[21] which both suffer from some disadvantages such as the imprecision with asymmetric and polydentate ligands or for solid angles, only providing a picture of the ligand in a frozen state.[21] In contrast, the "exact cone angle method"[21] is a more convenient technique for determining exact cone angles θ° via finding the most acute circular cone, containing all ligand atoms over a quadratic equation for the cosine of the cone angle. The size of the cone angle describes the ability of shielding an active metal center. Commonly used phosphane ligands show values around 200°.[22] Using the exact cone angle method,[21] Dipp and Tripp substituents used by Izod[6,16] have cone angles of 204 to 205°. For the diphosphastannylenes

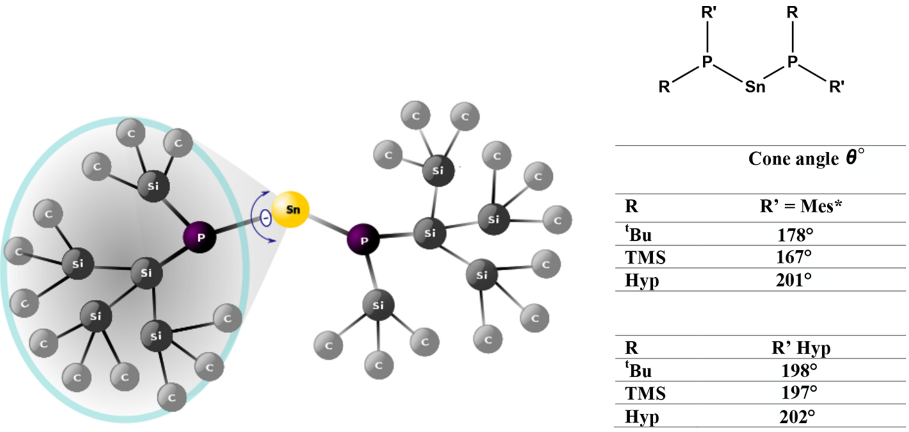

Cone angle θ°

R	R' = Mes*
^{t}Bu	178°
TMS	167°
Hyp	201°

R	R' Hyp
^{t}Bu	198°
TMS	197°
Hyp	202°

Figure 2. Schematic diagram of diphosphatetrylene cone angles.

Table 3. mPW1PW91/SDD DFT Calculated Data for the Global Minimum of $(Mes^*PR)_2Sn$

substituent	∑P(P)′ [deg]	P−R/P′−R [Å]	P−Sn/P′−Sn [Å]	P−Sn−P [deg]	Δ_{H-L} [eV]
^{t}Bu	325.4 (360.0)	2.00/1.98	2.70/2.52	104.2	3.05
TMS	347.0 (360.0)	2.34/2.35	2.36/2.35	110.3	3.25
Hyp	331.5 (359.9)	2.38/2.40	2.61/2.56	112.1	3.03

Table 4. mPW1PW91/SDD DFT Calculated Data for the Global Minimum of $(HypPR)_2Sn$

substituent	∑P(P)′ [deg]	P−R/P′−R [Å]	P−Sn/P′−Sn [Å]	P−Sn−P [deg]	Δ_{H-L} [eV]
^{t}Bu	309.7 (360.0)	1.96/1.94	2.68/2.51	102.0	3.16
TMS	328.0 (328.0)	2.35/2.36	2.58/2.61	98.82	3.11
Hyp	317.3 (358.9)	2.57/2.71	2.71/2.57	118.0	2.04

studied here, $(Mes^*RP)_2Sn$ and $(HypRP)_2Sn$, with R = H, Me, or Ph, values from 150 to 165° were obtained, making them less suitable for stabilizing monomeric diphosphatetrylenes. For the Hyp backbone, the TMS and ^{t}Bu ligands have values of 197 and 198°, respectively. In comparison, the Mes*backbone with R = TMS has a value for the cone angle of 167°, while ^{t}Bu with 178° might still be in a reasonable range (see Figure 2). In summary, the Hyp backbone in combination with a ^{t}Bu or TMS ligand seems to provide enough steric stabilization for the isolation of monomeric diphosphatetrylenes. Both backbone systems with special emphasis on R = ^{t}Bu, TMS, and Hyp, were considered for DFT calculations on diphosphastannylenes.

In a brief summary in Tables 3 and 4, the calculated data for the lowest energy minimum of each compound can be found (coordinates for all geometries are given in the Supporting Information). For every compound, four to five stable minimum geometries were located. At least one of those configurations had a planar P center, which indicates a higher overlap of the orbitals and therefore a stronger stabilization. In these conformers, one shorter P−Sn bond was detected, caused by the π-type interaction, which was also confirmed by NBO analyses, resulting in high delocalization energies (E_2 = 115−185 kcal/mol). Simultaneously, the P−Sn bond of the second P center was significantly elongated and shows only a weak interaction of this type. In the case of $(Mes^*RP)_2Sn$, all of the global minima, except for R = H, have one planar P atom. For R = ^{t}Bu, the global minimum is 15 kJ/mol more stable than the other minima. The Sn−P distances are 2.52 and 2.71 Å, with a P−Sn−P angle of 104.2°. The bond angle sums of the P atoms are 360 and 325°, respectively. For the TMS substituted compound, bond angle sums of 347.0 and 360.0° were detected. The P−Sn−P angle is 110.3°, slightly wider. Only for this compound a conformer with two almost planar P atoms, ∑P(P)′ = 355.6° (355.0°), was found. This conformer was the least stable one, with a ΔH of 20 kJ/mol. The Hyp substituted compound shows an increased P−Sn−P′ angle, because of the ligand size, which can be seen in Table 3.

The global minima of compounds $(HypPR)_2Sn$ have usually two pyramidal phosphorus centers. NBO analyses show in these cases interactions between the P lone pairs and the empty p-orbital on the Sn with lower delocalization energies (E_2 = 15−30 kcal/mol). Only for $(Hyp^tBuP)_2Sn$ and $(Hyp_2P)_2Sn$ a global minimum with a planar P center was detected. For $(Hyp^tBuP)_2Sn$, all of the minima are rather close in energy (ΔH = 3.1−16.5 kJ/mol). The global minimum structure has Sn−P distances of 2.51 and 2.69 Å, and the P bond angle sums are 360 and 309.7°. For the analogous compound with R = TMS, four minima were found only 1.7 to 3.4 kJ/mol less stable than the global minimum, and another four minima were located with ΔH = 8.8 to 24.8 kJ/mol. The global minimum is quite symmetric; both Sn−P distances are 2.59 Å, and both P atoms are pyramidal with a bond angle sum of 328°. A restricted scan for the planarization of one P center shows a very small barrier of approximately 5 kJ/mol. In the case of R = Hyp, there is a significant difference in the Sn−P distances, with 2.57 and 2.70 Å as seen in Table 4. This indicates reduced pyramidal environment on the second P atom, and indeed, the bond angles are 358.9 and 317.3°. The P−Sn−P bond angle (118°) is wider than in the TMS substituted compound (98.8°). The literature known silyl substituted compound isolated by Driess[10] has a P−Sn bond length of 2.567 Å and a P−Sn−P angle of 98.78°, similar to $(HypTMSP)_2Sn$ as seen in Table 4.

DOI: 10.1021/acs.organomet.8b00258

Scheme 1. Reaction Route to $Sn(PMes^{*}TMS)_2$

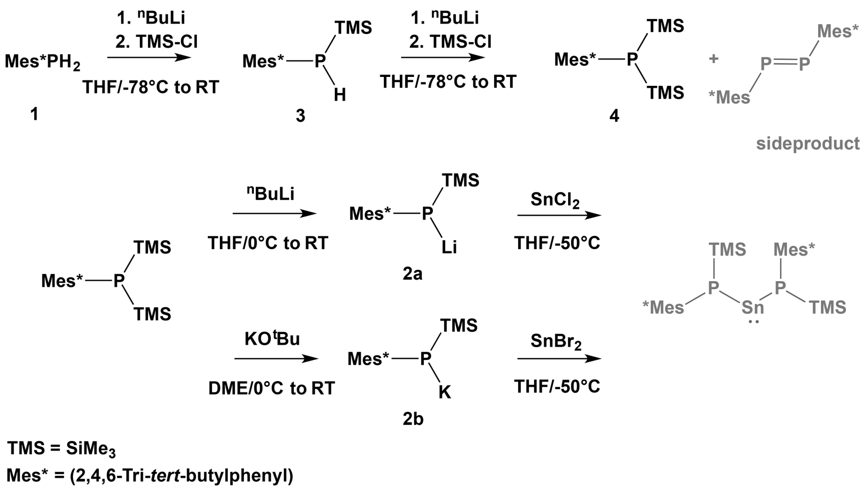

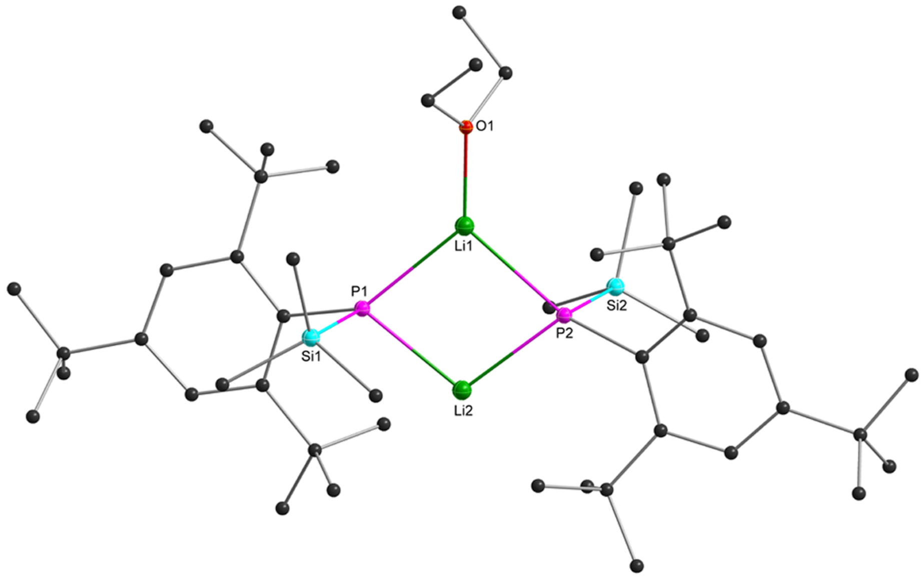

Figure 3. 2,4,6-Tris(*t*-butyl)phenyl trimethylsilyl lithium phosphanide **2a** obtained by X-ray diffraction analysis. All noncarbon atoms shown as 30% shaded ellipsoids. Hydrogen atoms have been omitted for clarity.

Concerning the NMR data, two shifts in the ^{31}P NMR should be detected if a compound has one pyramidal and one planar P center. These shifts differ in a quite remarkable manner. The shifts for the planar phosphorus atom are calculated to occur in our investigated stannylenes in a region from 22 to 52 ppm, while the pyramidal phosphorus centers resonate in the high field from −139 to −125 ppm. In the solid-state $^{31}P(^{1}H)$ MAS NMR spectra of the Dipp substituted compound isolated by Izod,[16] shifts at 95.8 ppm (P−Sn = 2620 Hz) and −66.2 ppm (P−Sn = 1180 Hz) occurred,[16] which matches their DFT calculations. In a toluene-d_8 solution, only a ^{31}P NMR peak at −25.1 ppm with a P−Sn coupling of 1300 Hz was found. This was attributed to small barriers of inversion.[16] Our calculations on a simpler model, $(PPh_2)_2Sn$, predict an inversion barrier of 2.4 kJ/mol.

As mentioned before, tetrylenes are interesting candidates for complementing transition metal compounds in catalytic processes. Particularly the activation of small molecules, such as H_2 and NH_3, arouses great interest. Schoeller[23] noted that HOMO−LUMO gaps, Δ_{H-L}, and singlet−triplet energy separations, ΔE_{S-T}, are essential in the reactions with small molecules. Smaller gaps lead to lower activation barriers and are therefore favorable.[16] Recently, it was mentioned[24] that by the use of phosphido ligands, the values for ΔE_{S-T} can be lowered to values below 63 kJ·mol^{-1}. In diaminotetrylenes, the values are around 88 kJ·mol^{-1} or higher. Literature known germylenes,[25] which were tested for H_2 activation, show HOMO−LUMO gap values from 3.4 to 3.6 eV. Compared with our results, we can see that in all Sn conformers seen in Tables 3 and 4, the HOMO−LUMO energy gaps are between 2.04 and 3.25 eV. If we take a closer look at our TMS substituted compounds, $(Mes^{*}PTMS)_2Sn$ and $(HypPTMS)_2Sn$, the absorption maximum for the Mes*compound is at 531 nm (red-purple), and the absorption maximum for the Hyp compound is at 676 nm (green blue). This indicates a smaller HOMO−LUMO gap for the $(HypPTMS_2)$-Sn, which could be confirmed with our DFT calculation; the Δ_{H-L} value for the Hyp compound is 3.11 eV, while the Mes*compound has a wider gap of 3.25 eV. The ΔE_{S-T} could be calculated with 128.5 kJ·mol^{-1} for $(Mes^{*}PTMS)_2Sn$ and 178.7 kJ·mol^{-1} for $(HypPTMS)_2Sn$. This makes these compounds ideal candidates for the activation of small

DOI: 10.1021/acs.organomet.8b00258
Organometallics XXXX, XXX, XXX−XXX

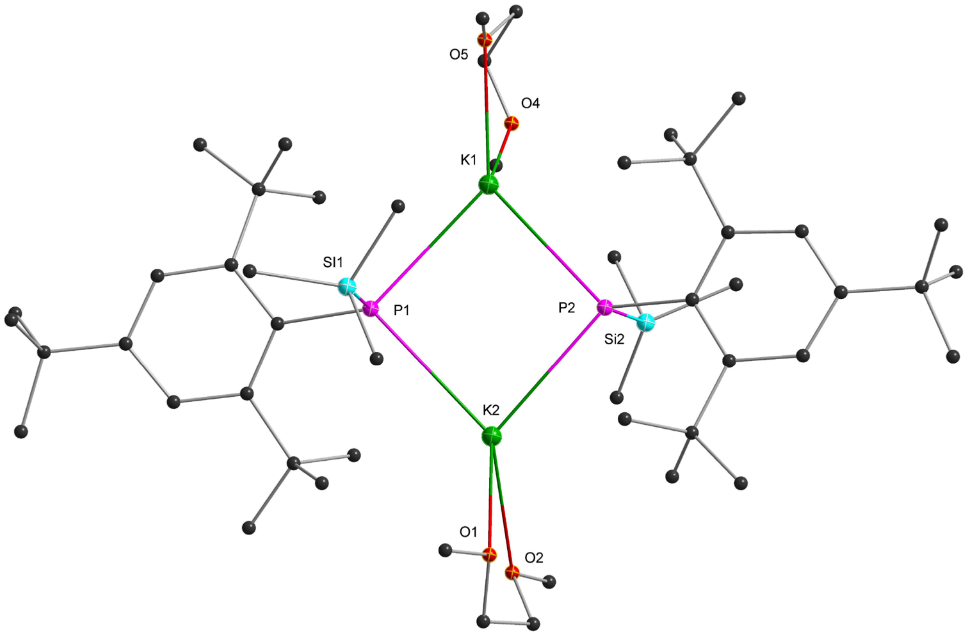

Figure 4. Structure of 2,4,6-Tris(*t*-butyl)phenyl trimethylsilyl potassium phosphanide]·DME **2b** obtained by X-ray diffraction analysis. All noncarbon atoms shown as 30% shaded ellipsoids. Hydrogen atoms have been omitted for clarity.

molecules. For the purpose of employing the insight gained from the calculations, we have chosen to apply the ligands ^{t}Bu and TMS for the synthesis of stable diphosphastannylenes in the form of Mes*RP−Sn−PRMes*and HypRP−Sn−PRHyp.

Experimental Approach. Mes*PH_2 (or supermesityl-PH_2) **1** and $(SiMe_3)_3Si-PH_2$[18] ($HypPH_2$) were chosen as convenient synthetic starting points in the synthesis of silylphosphanes, which can act as stabilizing ligands for diphosphatetrylenes. The lithiation of Mes*PH_2 **1** with ^{n}BuLi is well-known and yields the phosphanide Mes*PHLi. Straightforward salt elimination reaction with TMS-Cl yields the silaphosphane Mes*P(TMS)H **3**. A subsequent reaction with ^{n}BuLi and a salt elimination reaction with TMS-Cl leads to Mes*$P(TMS)_2$ **4**. The deprotonation reaction with ^{n}BuLi can also yield the diphosphene, a common side product (see Scheme 1).[26]

A reaction of Mes*$P(TMS)_2$ seems more complicated; however, reaction of **4** with ^{n}BuLi causes an almost quantitative (>99%) abstraction of one trimethylsilyl group, resulting in a clean lithium phosphanide **2a**. Si−P cleavage by ^{n}BuLi, as well as lithiation of primary and secondary phosphanes, is a well-known reaction. However, solid-state structures of **2a** and **2b** have not been reported to date. Crystals suitable for X-ray diffraction analysis of these were gained from a mixture of *n*-hexane and toluene (see Figures 3 and 4). A P−C bond length was observed with a length of 1.872 Å for the lithium phosphanide **2a** and 1.887 Å for the potassium phosphanide **2b**; the values for the P−Si bond (2.226 and 2.211 Å) are in a reasonable region. Both phosphanides crystallize as dimers consisting of two metal atoms bridged by two Mes*TMSP ligands in a P−M−P−M central ring (M = Li, K). In the case of **2a**, one Li coordination center is saturated by ether, while the second Li atom is stabilized by agostic interactions from the *t*-butyl groups of the Mes*ligand, with a coordination number of 2. The values for these Li···H−C contacts are within reported values for a Li···H−C (2.140, 2.365, and 2.745 Å) agostic interaction.[27] The P−Li bond lengths are 2.505 and 2.412 Å, comparable to the literature known lithium phosphanide $[LiPMes_2)(OEt_2)]_2$,[28] with P−Li bonds of 2.483 and 2.479 Å. In the case of the potassium phosphanide **2b**, each metal atom is coordinated to DME. The P−K bond lengths are 3.264 and 3.228 Å, comparable to the literature known P_3K bridged [3]ferrocenophane.[29] This compound has P−K bond lengths of 3.581 and 3.333 Å. The K···H−C contacts are as well within reported values for a K···H−C (2.845, 3.062, 3.101, 3.238 Å) agostic interaction.

The attempted tetrylene synthesis via reaction of Mes*PHosphanide with the corresponding Sn(II) halides ($SnCl_2$, $SnBr_2$) yielded a dark red solution and a red-brown precipitate. Further interpretation of this precipitate was difficult because of the poor solubility in any common solvent. The reaction solution was further analyzed via NMR. A ^{31}P signal at −392.1 ppm and a ^{119}Sn signal at 1292 ppm were detected. The red solution was stored at reduced temperature in order to gain crystals for a structure determination. Two kinds of crystals could be isolated. Apart from yellow crystals, which were analyzed to be Mes*−P = P−Mes*, a quite common side product in the reaction of lithium silylphosphides with halides,[30,31] small red crystals were formed. Unfortunately, X-ray diffraction analysis of these was not possible because of poor crystal quality.

In the literature, an NMR pattern similar to ours was found for a compound isolated by Westerhausen,[32] a tin−phosphorus cubane with Si^tBu_3 groups on P. It shows a ^{31}P signal at −452.1 ppm and a ^{119}Sn peak at 1234 ppm with a $^1J_{Sn-P}$ coupling constant of 788 Hz and a $^3J_{Sn-P}$ coupling constant of 84 Hz. Since this compound shows an upfield shift compared to our analyzed reaction solution, and carbon substituents on P were found to rather form cages, we suppose the formation of multinuclear Sn−P cage structures as mentioned by Wright.[33]

According to our calculations, $[HypPK-SiMe_3]$ is an ideal candidate for synthesizing a stable stannylene. The synthesis of $[HypPK-SiMe_3]$ has been described before[18] but was modified for this work. The replacement of toluene with 1,2-dimethoxyethane (DME) results in similarly high yields (>85%), making the addition of 18-crown-6 obsolete and the

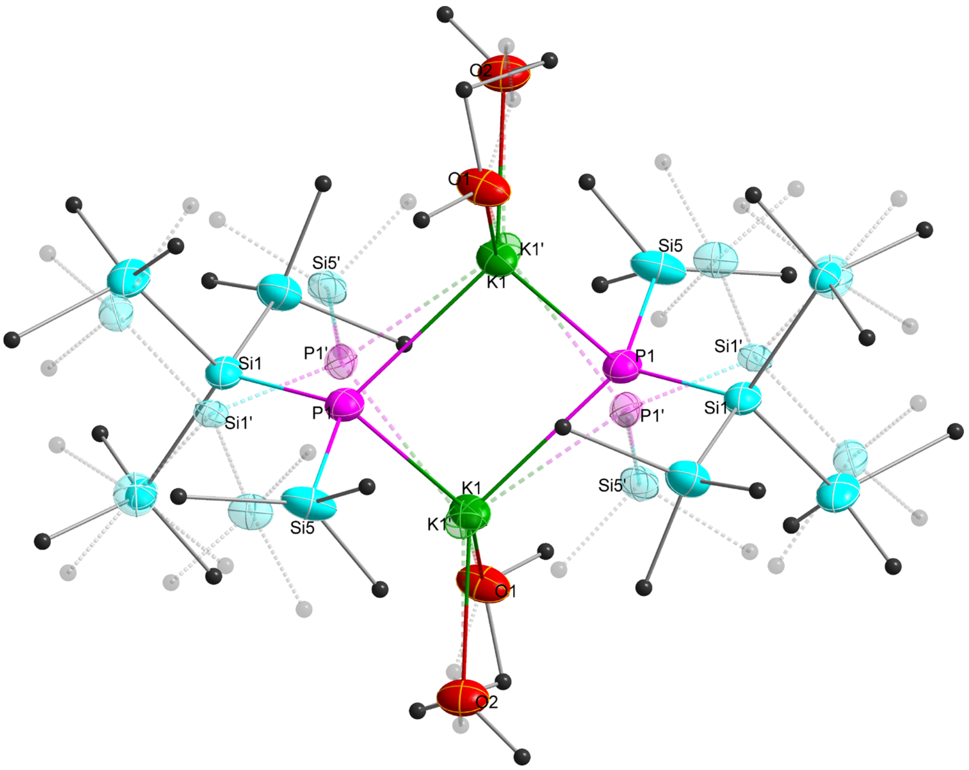

Figure 5. Disordered diagram of dipotassium salt **5** obtained by X-ray diffraction analysis. All noncarbon atoms shown as 30% shaded ellipsoids. Hydrogen atoms have been omitted for clarity.

Scheme 2. Reaction to $Sn(PTMSHyp)_2$

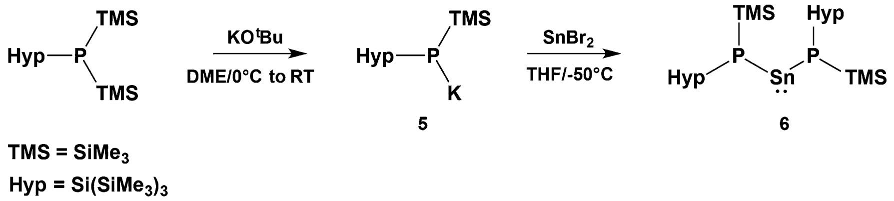

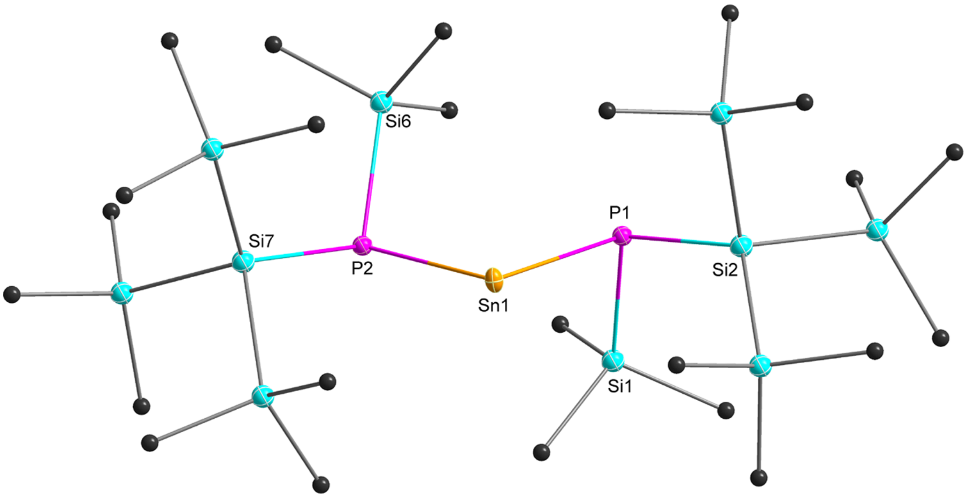

Figure 6. Solid-state structure of stannylene **6** obtained by X-ray diffraction analysis. All noncarbon atoms shown as 30% shaded ellipsoids. Hydrogen atoms have been omitted for clarity.

reaction able to be handled at room temperature. Crystals suitable for X-ray diffraction analysis were obtained after removal of the solvent and recrystallization from toluene with slow evaporation of the solvent at room temperature. Compound **5** crystallizes in a dimeric structural pattern, as seen in **2a** and **2b** with a four membered P−K−P−K central ring (see Figure 5). Each of the potassium ions is further stabilized via a dimethoxyethane molecule and agostic interactions to the methyl groups on the hypersilyl moiety. However, [HypPK−SiMe$_3$] displays whole molecule disorder (Supporting Information).

A reaction of [HypPK−SiMe$_3$] **5** in diethyl ether with tin(II)bromide diluted in THF (see Scheme 2) led to an immediate change of color to a rich emerald green. After replacement of the solvents with toluene and filtration, dark green needles were obtained at low temperatures (−30 °C). Analysis via X-ray diffraction gave the molecular structure of a novel diphosphastannylene [HypP−(SiMe$_3$)]$_2$Sn (see Figure 6) with two pyramidal P centers as predicted by DFT calculations. There are neither solvent molecules coordinating to the stannylene nor can any agostic intramolecular or intermolecular interactions be observed. In accordance to our calculations at the level of density functional theory (M06L/IGLO-II//mPW1PW91/SDD), a predicted absorption at 676 nm for the donor free stannylene, resulting in a green color, was observed. If a solvent molecule would have been coordinated to the metal center, this would have a direct influence on the HOMO−LUMO gap, resulting in an absorption at 495 nm. A UV/vis value was measured at 665 nm for this compound. Also in agreement with our calculated data (see Table 5), the Sn−P bond lengths and angles match the experimentally observed values. Compound **6** has Sn−P bond lengths of 2.53 and 2.56 Å and a P−Sn−P angle of 98.96°, resulting in a v-shape. These values are similar to those of Driess' compounds, which have P−Sn bond lengths of 2.57 Å and a P−Sn−P angle of 98.78°.[10]

Table 5. mPW1PW91/SDD DFT Calculated and Experimental Data for the Monomeric Diphosphastannylene 6

bond lengths	exp. [Å]	calc. [Å]
P1−Sn	2.53	2.59
P2−Sn	2.56	2.60
bond angles [deg]		
$\Sigma\alpha$(P) [deg]	306.1/321.4	328.0/328.0
P−Sn−P	98.95(6)	101.0

Compound **6** shows a downfield ^{119}Sn shift at 1467 ppm (see Figure 7), comparable to the compound isolated by Driess with a ^{119}Sn shift of 1551 ppm and a ${}^1J_{^{119}\text{Sn}-\text{P}}$ coupling constant of 1682 Hz. As expected for a tin atom substituted by two phosphorus moieties, the signal of **6** is a triplet with a ${}^1J_{^{119}\text{Sn}-\text{P}}$ coupling constant of 1486 Hz (see Figure 8), where our DFT calculations predict coupling constants of 1517 Hz.[10] The ${}^1J_{^{119}\text{Sn}-\text{P}}$ coupling, as well as the slightly smaller ${}^1J_{^{117}\text{Sn}-\text{P}}$ (1423 Hz) coupling, can also clearly be observed via ^{31}P NMR spectroscopy (see Figure 8). These coupling constants are considerably larger than those reported for Sn−P single bonds (700−1000 Hz)[10] and also larger than the coupling constants found for ligands in dimeric stannylenes (∼1000−1200 Hz).[8] A tin ferrocenophane dimer[34] shows a ^{119}Sn shift at +418 ppm with ${}^1J_{\text{Sn}-\text{P}}$ coupling constants of 702 Hz for the more deshielded P and another ${}^1J_{\text{Sn}-\text{P}}$ coupling constant of 1179 Hz for the phosphorus nucleus resonating at higher field,[34] showing that coupling constants for dimeric compounds are in between (700−1200 Hz).

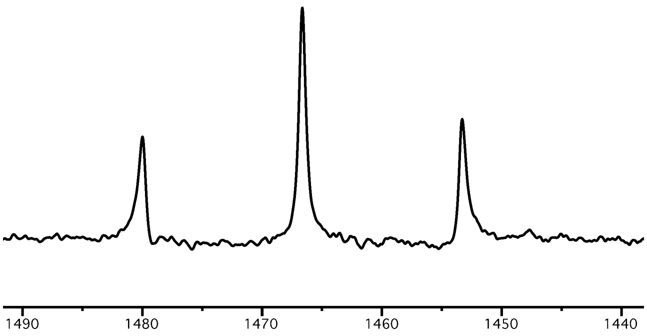

Figure 7. ^{119}Sn NMR resonance of **6** in the lowfield region.

Compound **6** has two pyramidal P centers and shows a sharp ^{31}P peak at −104.9 ppm, in agreement with our calculated data of −125 ppm.

This matches the data for comparable literature known compounds,[10] with ^{31}P shifts at −102.5 and −121.5 ppm. **6** has two stereogenic centers. The molecular structure and the calculated minimum structures with $\Delta H \leq 3$ kJ/mol are D,L-conformations. In solution a mixture of D,L- and *meso*-forms cannot be entirely ruled out, although the ^{119}Sn and the ^{31}P NMR peaks are quite sharp with line widths at half height of 37 and 3.5 Hz, respectively.

Studies concerning the proposed reactivity toward small molecules, such as H_2 or NH_3, are ongoing.

Conclusion. Through DFT calculations, a series of phosphorus ligands with different characteristics, such as size, steric demand, and type of substituent (aryl, alkyl, silyl) were evaluated for their ability to stabilize low valent tin(II) compounds. The effect of various substituents (H, Me, ^{t}Bu, Ph, TMS, Hyp = (Si(SiMe$_3$)$_3$)) on the pyramidalization of the phosphorus center were explored. In addition, the steric demand of these substituents was evaluated through exact cone angle determinations. The most promising substituents on (Mes*PR)$_2$Sn and (HypPR)$_2$Sn (R = ^{t}Bu, TMS, Hyp) were used in calculating the structures and HOMO−LUMO gap, giving an idea on their reactivity. Our combination of calculations and synthetic results indicate that the intramolecular stabilization via formation of a Sn═P double bond is less important than previously considered. NBO analysis showed that in conformers with one planar P center, strong π-type interactions occur. At the same time, the second P center is considerably weakened as expressed by an elongation of the P−Sn bond. Consequently, steric shielding needs to be increased to ensure stabilization. In case of two pyramidal P centers, simultaneous interaction between the lone pair of both P centers with the empty p-orbital of the Sn is found but yields comparably low delocalization energies. Calculations for (Mes*PTMS)$_2$Sn reveal conformers with planar P centers and a cone angle of 176°, which according to the literature should lead to the isolation of stable stannylene species. Experimentally, however, the use of this substituent combination did not give the desired results. In contrast, the combination of Hyp and TMS on the phosphorus centers does not have planar P atoms but has a larger steric demand with a cone angle of 197°. This led to a novel stable tin(II) species, (Hyp*PTMS)$_2$Sn, confirmed by experimental and calculated data. The solid-state structure shows no donor coordination to the metal center and no further interactions.

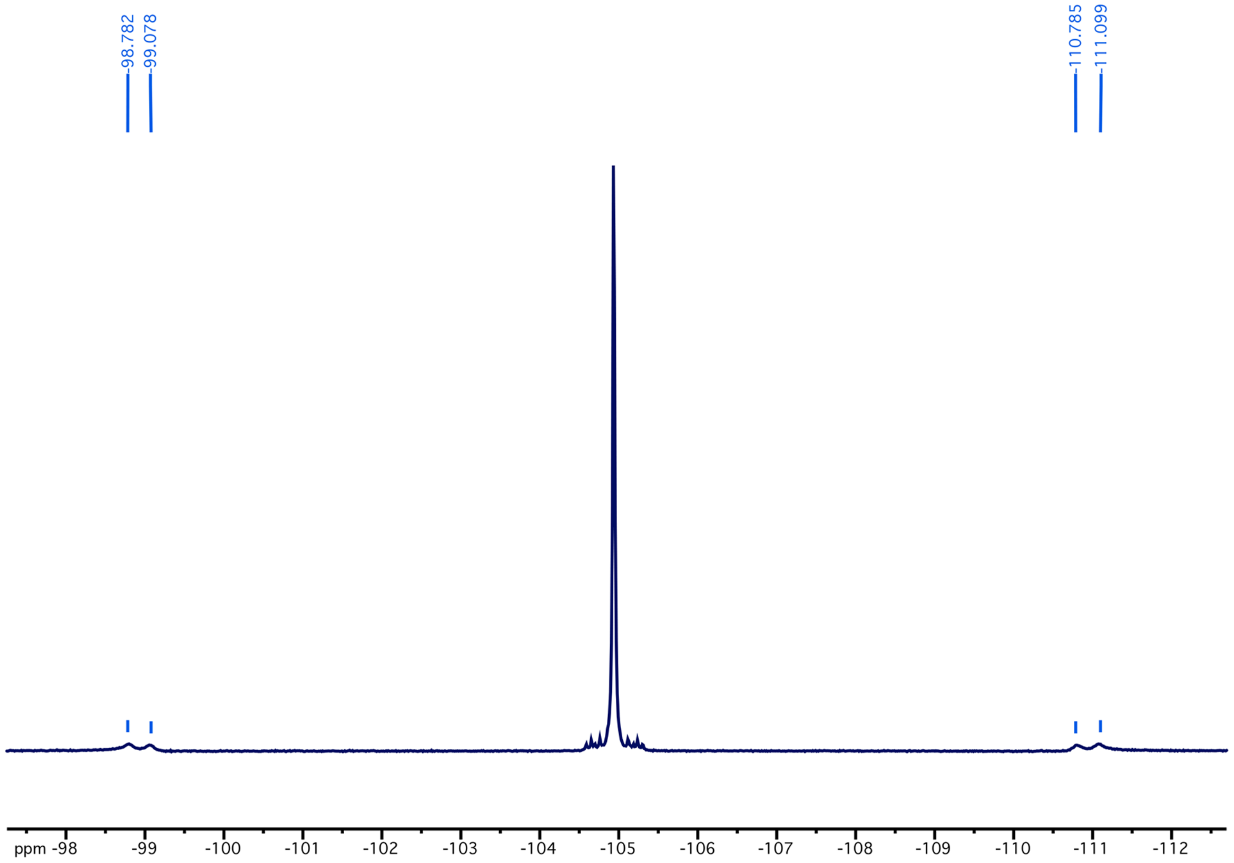

Figure 8. ^{31}P NMR resonance of **6**.

EXPERIMENTAL SECTION

General Procedures. All reactions, unless otherwise stated, were carried out using either standard Schlenk line techniques or in a glovebox under nitrogen atmosphere. All dried and deoxygenated solvents were obtained from a solvent drying system (Innovative Technology, Inc.). C_6D_6 has been destilled over sodium and stored under nitrogen atmosphere. *n*-Butyl lithium and potassium *tert*-butylate were bought from Aldrich and used as delivered. Dichlorotetramethyldisilane has been prepared following standard procedures.[35] HypP(SiMe$_3$)K **5** was prepared following procedures previously published.[18,19]

Because of the air, moisture, and, in the case of the stannylene, light, sensitivity of our compounds, we were unable to obtain meaningful elemental analysis results. This is a common problem observed in tin(II) species and alkaline metal complexes. Alkaline compounds, such as the reported phospanides, were already described before to be extremely reactive, and immediate decomposition at room temperature is very likely.[36,37]

The purity of all reported compounds was established by the absence of impurities, detected by NMR measurement for all nuclei (^{1}H, ^{13}C, ^{29}Si, ^{31}P, and ^{119}Sn NMR).

Computational Details. All calculations have been carried out using the Gaussian09 program package[38] on a computing cluster with blade architecture. For all calculations except calculations of magnetic shielding, the mPW1PW91 hybrid functional[39] was used. Magnetic shielding was calculated using the M06L[40] pure functional as implemented in Gaussian09. For optimizations and calculation of frequencies, the basis set combination denoted by SDD as implemented in Gaussian09[38]was used. For calculation of UV/vis absorptions and NMR magnetic shielding, the all electron IGLO-II[41] basis set was used. The magnetic shielding of H_3P0_4 ($\sigma^{31}P = 624.7$) was used as reference.

NMR. ^{1}H (300.2 MHz), ^{13}C (75.5 MHz), ^{29}Si (59.6 MHz), ^{119}Sn (111.8 MHz), and ^{31}P (121.5 MHz) NMR spectra were recorded on a Mercury 300 MHz spectrometer from Varian at 25 °C. Chemical shifts are given in parts per million (ppm) relative to TMS ($\delta = 0$ ppm) regarding ^{1}H, ^{13}C, and ^{29}Si. Coupling constants (J) are reported in hertz (Hz). All NMR spectra were measured in C_6D_6.

X-ray Diffraction. All crystals suitable for single crystal X-ray diffractometry were removed from a vial or a Schlenk under N_2 and immediately covered with a layer of silicone oil. A single crystal was selected, mounted on a glass rod on a copper pin, and placed in the cold N_2 stream provided by an Oxford Cryosystems cryostream. XRD data collection was performed for compounds **2a**, **2b**, **5**, and **6** on a Bruker APEX II diffractometer with use of an Incoatec microfocus sealed tube with Mo Kα radiation ($\gamma = 0.71073$ Å) and a CCD area detector. Empirical absorption corrections were applied using SADABS or TWINABS.[42,43] The structures were solved with use of the intrinsic phasing option in SHELXT and refined by the full-matrix least-squares procedures in SHELXL.[44−46] The space group assignments and structural solutions were evaluated using PLATON.[47,48] Non-hydrogen atoms were refined anisotropically. All other hydrogen atoms were located in calculated positions corresponding to standard bond lengths and angles and refined using a riding model. Disorder as observed for compounds **2a**, **2b**, and **5** was handled by modeling the occupancies of the individual orientations using free variables to refine the respective occupancies of the affected fragments (PART).[49] In some cases, the similarity SAME restraint, the similar-ADP restraint SIMU, and the rigid-bond restraint DELU, as well as the constraints EXYZ and EADP, were used in modeling disorder to make the ADP values of the disordered atoms more reasonable. In some cases, the distances between arbitrary atom pairs were restrained to possess the same value using the SADI instruction, and in some cases, distance restraints (DFIX) to certain target values were used. In some tough cases of disorder, anisotropic U^{ij} values of the atoms were restrained (ISOR) to behave more isotropically. Disordered positions for the coordinated ether in 2,4,6-tris(*t*-butyl)phenyl trimethylsilyl lithium phosphanide **2a** were refined using 70/30 split positions. Disordered positions for a $SiMe_3$ group, a coordinated DME, and a methyl group in a *t*-butyl group in compound [2,4,6-tris(*t*-butyl)phenyl trimethylsilyl potassium phosphanide]·DME **2b** were refined using 50/50, 50/50, and 55/45 split positions, respectively. In addition to poor crystal quality for compound [HypP($SiMe_3$)K·DME] **5**, resulting in high RINT values and low bond precision, whole molecule disorder was refined using 60/40 split positions. Despite multiple least-squares refinement cycles, proper convergence of the refinement was not achieved and attributed to poor crystal quality and not incorrect atom assignments. All agostic interactions for presented compounds fall within reported values[27,50] and are based on a Cambridge Structural Database search.[51] CCDC 1838937−1838940 contain the supplementary crystallographic data for compounds **2a**, **2b**, **5**, and **6** respectively. These data can be obtained free of charge from The Cambridge Crystallographic Data Centre via www.ccdc.cam.ac.uk/data_request/cif.

Crystallographic data and details of measurements and refinement for compounds **2a**, **2b**, **5**, and **6** can be found in the Supporting Information.

Synthesis. *Synthesis of 2,4,6-Tris(t-butyl)phenyl Trimethylsilyl Lithium Phosphanide* ***2a***. 2,4,6-Tris(*t*-butyl)phenyl trimethylsilyl phosphane (0.40 g, 1.14 mmol) was dissolved in 5 mL of THF. 0.82 mL of 1.6 M *n*-butyl lithium (1.15 eq, 1.31 mmol) in hexanes was added dropwise at RT. The color of the reaction solution changed to yellow, and the solution was stirred for an additional 2 h. After evaporation of all volatile components, the solid residue was redissolved in *n*-hexane. After 1 week at −30 °C, crystals suitable for X-ray diffraction analysis can be isolated from this solution. Yield: 0.19 g, 42%. ^1H NMR (C_6D_6, 293 K): δ 0.15 ppm (9H, d, $SiMe_3$, $^3J_{HP}$ = 3.9 Hz), 3.66 ppm (18H, o-*t*-Bu) 3.91 ppm (9H, p- *t*-Bu) 7.16 ppm (2H, d, arom., $^4J_{HP}$ = 1.8 Hz). ^{13}C NMR (C_6D_6, 293 K): δ 4.33 ppm ($SiMe_3$, d, $^2J_{CP}$ = 12.8 Hz), 31.2 ppm (o-C*Me*$_3$, d, $^3J_{CP}$ = 8.1 Hz), 33.3 ppm (o-CMe_3, d, $^4J_{CP}$ = 8.8 Hz), 34.7 ppm (p-C*Me*$_3$), 38.8 ppm (p-CMe_3), 118.7 ppm (arom., d, $^2J_{CP}$ = 3.7 Hz), 121.1 ppm (arom., d, $^2J_{CP}$ = 4.25 Hz), 149.8 ppm (arom.), 157.6 ppm (arom.). ^{29}Si NMR (C_6D_6, 293 K): δ 7.94 ppm (d, $^1J_{SiP}$ = 21.8 Hz). ^{31}P NMR (C_6D_6, 293 K): δ −151.4 ppm.

Synthesis of [2,4,6-Tris(t-butyl)phenyl Trimethylsilyl Potassium Phosphanide]·DME ***2b***. 2,4,6-Tris(*t*-butyl)phenyl bis-trimethylsilyl phosphane (0.13 g, 0.28 mmol) was dissolved in 3 mL of DME. A solution of 0.035 g (0.31 mmol) of KO*t*Bu in 2 mL of DME was added dropwise at RT. The colorless solution changed to yellow immediately and was subsequently stirred for 2 h. After evaporation of all volatile components, the residue was redissolved in *n*-hexane. After 1 week at −30 °C, crystals suitable for X-ray diffraction analysis could be isolated from this solution. Yield: 0.11 g, 82%. ^1H NMR (C_6D_6, 293 K): δ 0.24 ppm (9H, d, $SiMe_3$, $^3J_{HP}$ = 3.6 Hz), 1.40 ppm (9H, p-*t*-Bu), 1.99 ppm (18H, o- *t*-Bu), 3.00 ppm (4H, DME CH_2), 7.11 ppm (2H, broad s, arom.). ^{13}C NMR (C_6D_6, 293 K): δ 4.0 ppm ($SiMe_3$, d, $^2J_{CP}$ = 13.4 Hz), 31.2 ppm (o-C*Me*$_3$, d, $^3J_{CP}$ = 8.1 Hz), 33.4 ppm (o-CMe_3, d, $^4J_{CP}$ = 8.8 Hz), 34.5 ppm (p-C*Me*$_3$), 38.5 ppm (p-CMe_3), 58.3 ppm (DME), 71.2 ppm (DME), 118.8 ppm (arom., d, $^2J_{CP}$ = 12.8 Hz), 118.9 ppm (arom.), 143.4 ppm (arom.), 156.0 ppm (arom.). ^{29}Si NMR (C_6D_6, 293 K): δ −0.83 ppm (d, $^1J_{SiP}$ = 58.4 Hz). ^{31}P NMR (C_6D_6, 293 K): δ −143.1 ppm.

Synthesis of [HypP(SiMe$_3$)K·DME] ***5***. HypP($SiMe_3$)$_2$ (1.00 g, 2.4 mmol) and KO^{t}Bu (0.28 g, 2.5 mmol) were brought into a Schlenk flask under inert atmosphere. Dissolution of the solid, colorless educts in 6 mL of 1,2-dimethoxyethane (DME) at 0 °C led to an immediate change of color to intense yellow. After the mixture was vigorously stirred for 24 h, all volatile components were removed under reduced pressure. The residue was redissolved in a mixture of pentane and toluene. Crystals suitable for X-ray diffraction analysis were obtained from this solution at −30 °C. Yield: 0.98 g, 87%. ^1H NMR (C_6D_6, 293 K): δ 0.09 ppm (27H, s, (*Me*$_3$Si)$_3$Si), 0.17 ppm (9H, d, $SiMe_3$, $^3J_{HP}$ = 3.6 Hz), 1.47 ppm (9H, p-*t*-Bu) 2.00 ppm (18H, o-*t*-Bu), 2.96 ppm (6H, DME CH_3), 3.00 ppm (4H, DME CH_2). ^{13}C NMR (C_6D_6, 293 K): δ 2.0 ppm (9C, d, $^3J_{CP}$ = 12.2 Hz, (*Me*$_3$Si)$_3$Si), 8.5 ppm (3C, d, $^2J_{CP}$ = 11.6 Hz, *Me*$_3$Si). ^{29}Si NMR (C_6D_6, 293 K): δ −94.8 ppm (Si, d, $^1J_{SiP}$ = 118.2 Hz, (Me_3Si)$_3$*Si*), −14.14 ppm (3Si, d, $^2J_{SiP}$ = 12.6 Hz (Me_3*Si*)$_3$Si), −0.53 ppm (1Si, d, $^1J_{SiP}$ = 78.9 Hz, Me_3*Si*). ^{31}P NMR (C_6D_6, 293 K): δ −355.8 ppm.

Synthesis of [HypP(SiMe$_3$)]$_2$Sn ***6***. A solution of HypP(SiMe3)K·DME (0.92 g, 1.91 mmol) in 6 mL of DME was cooled to −50 °C and slowly added to a cooled (−50 °C) suspension of $SnBr_2$ (0.27g, 0.96 mmol) in 10 mL of THF in a 100 mL Schlenk flask via cannula under vigorous stirring. Upon addition, the reaction solution turned to dark green. The reaction was allowed to warm up to room temperature and was vigorously stirred for 16 h. After removal of solvents under reduced pressure, the residue was dissolved in pentane and filtered from salts. Crystals suitable for X-ray diffraction analysis were obtained from pentane at −30 C. Yield: 0.72 g. ^1H NMR (C_6D_6, 293 K): δ 0.35 ppm (27H, broad s, (*Me*$_3$Si)$_3$Si), 0.50 ppm (9H, d, $^3J_{HP}$ = 3.6 Hz, *Me*$_3$Si). ^{13}C NMR (C_6D_6, 293 K): δ 2.7 ppm (18C, broad s, (*Me*$_3$Si)$_3$Si), 6.5 ppm (6C, dd, $^2J_{CP}$ = 7.2 Hz, $^4J_{CP}$ = 6.0 Hz, *Me*$_3$Si). ^{29}Si NMR (C_6D_6, 293 K): δ −91.5 ppm (2Si, dd, $^1J_{SiP}$ = 79.6 Hz, $^3J_{SiP}$ = 10.8 Hz, (Me_3Si)$_3$*Si*), −9.9 ppm (6Si, dd, $^2J_{SiP}$ = 5.0 Hz, $^4J_{SiP}$ = 3.8 Hz, (Me_3*Si*)$_3$Si), 6.1 ppm (2Si, dd, $^1J_{SiP}$ = 51.5 Hz, $^3J_{SiP}$ = 5.0 Hz, Me_3*Si*). ^{31}P NMR (C_6D_6, 293 K): δ −104.9 ppm ($^1J^{117}{}_{SnP}$ = 1423 Hz, $^1J^{119}{}_{SnP}$ = 1486 Hz); ^{119}Sn NMR (C_6D_6, 293 K): δ 1467 ppm ($^1J^{117}{}_{SnP}$ = 1486 Hz)

■ ASSOCIATED CONTENT

Ⓢ Supporting Information

The Supporting Information is available free of charge on the ACS Publications website at DOI: 10.1021/acs.organomet.8b00258.

S1_Bonds and angles 1: Selected bond lengths and angles for presented and reference solid-state diphosphastannylene structures; S2_Bonds and angles 2: Selected bond lengths and angles for presented phosphanide structures **2a**, **2b**, **5**; S3_Crystallographic data: Data and details of measurements for compounds **2a**, **2b**, **5**, **6**; S4_DFT: mpw1pw91/sdd calculated data of various conformers of diphosphastannylenes (HypPR)$_2$Sn and (Mes*PR)$_2$Sn); S5_NMR: ^1H, ^{31}P, ^{29}Si, ^{119}Sn, and ^{13}C NMR of presented compounds reported in the Experimental section; S5_Crystallographic data: Data and details of measurements for compounds **2a**, **2b**, **5**, **6** (PDF)

S7_DFT.xyz: Cartesian coordinates (.xyz) of all investigated compounds (XYZ)

Accession Codes

CCDC 1838937−1838940 contain the supplementary crystallographic data for this paper. These data can be obtained free of charge via www.ccdc.cam.ac.uk/data_request/cif, or by emailing data_request@ccdc.cam.ac.uk, or by contacting The Cambridge Crystallographic Data Centre, 12 Union Road, Cambridge CB2 1EZ, UK; fax: +44 1223 336033.

■ AUTHOR INFORMATION

Corresponding Authors

*E-mail: elisabeth.schwarz@tugraz.at; Phone: +43 316 873 32101 (E.S.)

*E-mail: michaela.flock@tugraz.at; Phone: +43 316 873 32101 (M.F.)

ORCID

Elisabeth Schwarz: 0000-0002-9846-4107

Michaela Flock: 0000-0002-2799-1479

Notes

The authors declare no competing financial interest.

■ REFERENCES

(1) Arduengo, A. J.; Harlow, R. L.; Kline, M. A stable crystalline carbene. *J. Am. Chem. Soc.* **1991**, *113*, 361−363.

(2) Martin, D.; Baceiredo, A.; Gornitzka, H.; Schoeller, W. W.; Bertrand, G. A Stable P-Heterocyclic Carbene. *Angew. Chem., Int. Ed.* **2005**, *44*, 1700−1703.

(3) Hitchcock, P. B.; Lappert, M. F.; Misra, M. C. Homoleptic, three-co-ordinate group 8c noble metal(0) complexes having GeII or SnII ligands, $[M\{M'(NR_2)2\}_3]$(M = Pd or Pt, M′= Ge or Sn, R = $SiMe_3$), and the X-ray structure of one of them (M = Pd, M′= Sn). *J. Chem. Soc., Chem. Commun.* **1985**, *0*, 863−864.

(4) Veith, M. Cyclic Nitrogen Derivatives of Tetra- and Divalent Tin. *Angew. Chem., Int. Ed. Engl.* **1975**, *14*, 263−264.

(5) Iovkova-Berends, L.; Seiger, M.; Westfeld, T.; Hoffmann, A.; Herres-Pawlis, S.; Jurkschat, K. Extending the Family of N-Heterocyclic Heavy Carbene Analogues: Synthesis and Crystal and Molecular Structures of $MeN[CH_2C(O)N(R)]_2Sn$ (R = $Me_2NCH_2CH_2$, $PhCH_2$, Me_3CCH_2). *Eur. J. Inorg. Chem.* **2013**, *2013*, 5836−5842.

(6) Izod, K.; Rayner, D. G.; El-Hamruni, S. M.; Harrington, R. W.; Baisch, U. Stabilization of a Diphosphagermylene through p-p Interactions with a Trigonal-Planar Phosphorus Center. *Angew. Chem., Int. Ed.* **2014**, *53*, 3636−3640.

(7) Kapp, J.; Schade, C.; El-Nahas, A. M.; von Ragué Schleyer, P. Die π-Donorfähigkeit schwerer Elemente ist nicht geringer. *Angew. Chem.* **1996**, *108*, 2373−2376.

(8) du Mont, W.-W.; Kroth, H.-J. Dimeric Bis(di-tert-butylphosphino)stannanediyl: A Cyclic Phosphorus-Tin Ylide. *Angew. Chem., Int. Ed. Engl.* **1977**, *16*, 792−793.

(9) Goel, S. C.; Chiang, M. Y.; Rauscher, D. J.; Buhro, W. E. Comparing the properties of homologous phosphido and amido complexes: synthesis and characterization of the disilylphosphido complexes $\{M[P(SiMe_3)_2]_2\}_2$ where M = zinc, cadmium, mercury, tin, lead and manganese. *J. Am. Chem. Soc.* **1993**, *115*, 160−169.

(10) Driess, M.; Janoschek, R.; Pritzkow, H.; Rell, S.; Winkler, U. Diphosphanyl- and Diarsanyl-Substituted Carbene Homologues: Germanediyls, Stannanediyls, and Plumbanediyls with Remarkable Electronic Structures. *Angew. Chem., Int. Ed. Engl.* **1995**, *34*, 1614−1616.

(11) Westerhausen, M.; Digeser, M. H.; Nöth, H.; Ponikwar, W.; Seifert, T.; Polborn, K. 2,5-Diphenyl-3,4-bis(trimethylsilyl)-1-phosphacyclopentadienide as a Ligand at Calcium, Strontium, and Tin(II). *Inorg. Chem.* **1999**, *38*, 3207−3214.

(12) Brym, M.; Francis, M. D.; Jin, G.; Jones, C.; Mills, D. P.; Stasch, A. Facile Transformations of a 1,3,5-Triphosphacyclohexadienyl Anion within the Coordination Sphere of Group 13 and 14 Elements: Synthesis of 1,3-Diphosphacyclopentadienyl Complexes and Phosphaorganometallic Cage Compounds. *Organometallics* **2006**, *25*, 4799−4807.

(13) Rivard, E.; Sutton, A. D.; Fettinger, J. C.; Power, P. P. Synthesis of the sterically congested diarylphosphines and and the monomeric Sn(II)-diphosphide. *Inorg. Chim. Acta* **2007**, *360*, 1278−1286.

(14) Izod, K.; McFarlane, W.; Allen, B.; Clegg, W.; Harrington, R. W. An Intramolecularly Base-Stabilized Diphosphagermylene and Two Unusual Germanium(II) Ate Complexes: A Structural, NMR, and DFT Study. *Organometallics* **2005**, *24*, 2157−2167.

(15) Řezníček, T.; Dostál, L.; Růžička, A.; Jambor, R. Diphosphastannylenes: Precursors for Phosphorus-Phosphorus Coupling? *Eur. J. Inorg. Chem.* **2012**, *2012*, 2983−2987.

(16) Izod, K.; Evans, P.; Waddell, P. G.; Probert, M. R. Remote Substituent Effects on the Structures and Stabilities of P = E π-Stabilized Diphosphatetrylenes $(R_2P)_2E$ (E = Ge, Sn). *Inorg. Chem.* **2016**, *55*, 10510−10522.

(17) Kira, M.; Ishida, S.; Iwamoto, T.; Kabuto, C. The First Isolable Dialkylsilylene. *J. Am. Chem. Soc.* **1999**, *121*, 9722−9723.

(18) Cappello, V.; Baumgartner, J.; Dransfeld, A.; Hassler, K. Monophosphanes and Diphosphanes with the Hypersilyl Substituent. *Eur. J. Inorg. Chem.* **2006**, *2006*, 4589−4599.

(19) Mueller, S. K.; Weinberger, G.; Schwarz, E.; Torvisco, A.; Dransfeld, A.; Fischer, R. C.; Hassler, K.; Flock, M. Synthesis and Crystal Structures of Novel Silylsubstituted Diphosphanes. *Inorg. Chim. Acta* **2014**, *423*, 517−523.

(20) Bruckmann, J.; Krüger, C. Tris(n-butyl)phosphine, Tris(tert-butyl)phosphine and Tris(trimethylsilyl)phosphine. *Acta Crystallogr., Sect. C: Cryst. Struct. Commun.* **1995**, *51*, 1152.

(21) Bilbrey, J. A.; Kazez, A. H.; Locklin, J.; Allen, W. D. Exact ligand cone angles. *J. Comput. Chem.* **2013**, *34*, 1189−1197.

(22) Immirzi, A.; Musco, A. A method to measure the size of phosphorus ligands in coordination complexes. *Inorg. Chim. Acta* **1977**, *25*, L41−L42.

(23) Frey, G. D.; Lavallo, V.; Donnadieu, B.; Schoeller, W. W.; Bertrand, G. Facile Splitting of Hydrogen and Ammonia by Nucleophilic Activation at a Single Carbon Center. *Science* **2007**, *316*, 439−441.

(24) Protchenko, A. V.; Bates, J. I.; Saleh, L. M. A.; Blake, M. P.; Schwarz, A. D.; Kolychev, E. L.; Thompson, A. L.; Jones, C.; Mountford, P.; Aldridge, S. Enabling and Probing Oxidative Addition and Reductive Elimination at a Group 14 Metal Center: Cleavage and Functionalization of E-H Bonds by a Bis(boryl)stannylene. *J. Am. Chem. Soc.* **2016**, *138*, 4555−4564.

(25) Paul, D.; Heins, F.; Krupski, S.; Hepp, A.; Daniliuc, C. G.; Klahr, K.; Neugebauer, J.; Glorius, F.; Hahn, F. E. Synthesis and Reactivity of Intramolecularly NHC-Stabilized Germylenes and Stannylenes. *Organometallics* **2017**, *36*, 1001−1008.

(26) Yoshifuji, M. Sterically protected organophosphorus compounds of unusual structures. *Pure Appl. Chem.* **2017**, *89*, 281−286.

(27) Scherer, W.; Sirsch, P.; Shorokhov, D.; McGrady, G. S.; Mason, S. A.; Gardiner, M. G. Valence-Shell Charge Concentrations and Electron Delocalization in Alkyllithium Complexes: Negative Hyperconjugation and Agostic Bonding. *Chem. - Eur. J.* **2002**, *8*, 2324−2334.

(28) Hey, E.; Raston, C. L.; Skelton, B. W.; White, A. H. *J. Organomet. Chem.* **1989**, *362*, 1−10.

(29) Isenberg, S.; Frenzel, L.-M.; Bruhn, C.; Pietschnig, R. Metallated [3]Ferrocenophanes Containing P_3M Bridges (M = Li, Na, K). *Inorganics* **2018**, *6*, 67.

(30) Sasaki, S.; Yoshifuji, M.; Inamoto, N. Reaction of lithium (2,4,6-tri-*tert*-butylphenyl)silylphosphides with haloforms. *Arkivoc* **2012**, *ii*, 15−23.

(31) Cowley, A.; Newman, T. Reaction of (Tri(trimethylsilyl)silyl) lithium with Halophosphines. A Novel Silicon-Halogen Exchange Reaction. *Organometallics* **1982**, *1*, 1412−1413.

(32) Westerhausen, M.; Krofta, M.; Wiberg, N.; Knizek, J.; Nöth, H.; Pfitzner, A. Tetrazinn(II)-und Bariumtrizinn(II)-tetrakis[μ3-tri-ter/-butyIsilylphosphan-diid]-Verbindungen mit einem Tetrametallatetraphosphacuban-Gerüst. *Z. Naturforsch., B: J. Chem. Sci.* **1998**, *53*, 1489−1493.

(33) McPartlin, M.; Melen, R.; Naseri, V.; Wright, D. Formation and Rearrangement of SnII Phosphanediide Cages. *Chem. - Eur. J.* **2010**, *16*, 8854−8860.

(34) Kargin, D.; Kelemen, Z.; Krekic, K.; Maurer, M.; Bruhn, C.; Nyulaszi, L.; Pietschnig, R. [3]Ferrocenophanes with the bisphosphanotetryl bridge: inorganic rings on the way to tetrylenes. *Dalton Trans.* **2016**, *45*, 2180−2189.

(35) Hengge, E.; Pletka, H. D.; Hoefler, F. Preparation and properties of amino disilanes. *Monatsh. Chem.* **1970**, *101*, 325.

(36) Nief, D.; Mercier, F.; Mathey, F. Reactions of (phosphine)-pentacarbonyltungsten.Synthesis of primary and secondary phosphines in the coordination sphere of tungsten. *J. Organomet. Chem.* **1987**, *328*, 349−355.

(37) Westerhausen, M.; Rotter, T.; Görls, H.; Birg, C.; Warchhold, M.; Nöth, H. Lithium Bis(triisopropylsilyl)phosphanide and its Pentacarbonyltungsten Adduct: Synthesis and Crystal Structures of the Dimer $[(thf)Li\text{-}P(Si\mathit{i}Pr_3)_2]_2$ and the Solvent-Separated Ion Pair $[(thf)_4Li]^+$ $[(OC)_5W\text{-}P(Si\mathit{i}Pr_3)_2]^-$. *Z. Naturforsch., B: J. Chem. Sci.* **2005**, *60*, 766.

(38) Frisch, M. J.; Trucks, G. W.; Schlegel, H. B.; Scuseria, G. E.; Robb, M. A.; Cheeseman, J. R.; Scalmani, G.; Barone, V.; Mennucci, B.; Petersson, G. A.; Nakatsuji, H.; Caricato, M.; Li, X.; Hratchian, H. P.; Izmaylov, A. F.; Bloino, J.; Zheng, G.; Sonnenberg, J. L.; Hada, M.; Ehara, M.; Toyota, K.; Fukuda, R.; Hasegawa, J.; Ishida, M.; Nakajima, T.; Honda, Y.; Kitao, O.; Nakai, H.; Vreven, T.; Montgomery, J. A., Jr.; Peralta, J. E.; Ogliaro, F.; Bearpark, M.; Heyd, J. J.; Brothers, E.; Kudin, K. N.; Staroverov, V. N.; Kobayashi, R.; Normand, J.; Raghavachari, K.; Rendell, A.; Burant, J. C.; Iyengar, S. S.; Tomasi, J.; Cossi, M.; Rega, N.; Millam, J. M.; Klene, M.; Knox, J. E.; Cross, J. B.; Bakken, V.; Adamo, C.; Jaramillo, J.; Gomperts, R.; Stratmann, R. E.; Yazyev, O.; Austin, A. J.; Cammi, R.; Pomelli, C.; Ochterski, J. W.; Martin, R. L.; Morokuma, K.; Zakrzewski, V. G.; Voth, G. A.; Salvador, P.; Dannenberg, J. J.; Dapprich, S.; Daniels, A. D.; Farkas, O.; Foresman, J. B.; Ortiz, J. V.; Cioslowski, J.; Fox, D. J. *Gaussian 09*, revision E.01; Gaussian, Inc.: Wallingford, CT, 2009.

(39) Adamo, C.; Barone, V. Exchange functionals with improved long-range behavior and adiabatic connection methods without adjustable parameters: The mPW and mPW1PW models. *J. Chem. Phys.* **1998**, *108*, 664.

(40) Zhao, Y.; Truhlar, D. G. A new local density functional for main-group thermochemistry, transition metal bonding, thermochemical kinetics, and noncovalent interactions. *J. Chem. Phys.* **2006**, *125*, 194101.

(41) Kutzelnigg, W.; Fleischer, U.; Schindler, M. *Deuterium and Shift Calculation*; NMR Basic Principles and Progress; Springer, 1991; Vol. *23*; p 165.

(42) Bruker *APEX2 and SAINT*; Bruker AXS Inc.: Madison, Wisconsin, USA, 2012.

(43) Blessing, R. H. An empirical correction for absorption anisotropy. *Acta Crystallogr., Sect. A: Found. Crystallogr.* **1995**, *51*, 33−38.

(44) Sheldrick, G. M. Phase annealing in *SHELX*-90: direct methods for larger structures. *Acta Crystallogr., Sect. A: Found. Crystallogr.* **1990**, *46*, 467−473.

(45) Sheldrick, G. M. A short history of *SHELX*. *Acta Crystallogr., Sect. A: Found. Crystallogr.* **2008**, *64*, 112−122.

(46) Sheldrick, G. M. *SHELXT* − Integrated space-group and crystal-structure determination. *Acta Crystallogr., Sect. A: Found. Adv.* **2015**, *71*, 3−8.

(47) Spek, A. L. Structure validation in chemical crystallography. *Acta Crystallogr., Sect. D: Biol. Crystallogr.* **2009**, *65*, 148−155.

(48) Spek, A. L. Single-crystal structure validation with the program *PLATON*. *J. Appl. Crystallogr.* **2003**, *36*, 7−13.

(49) Müller, P.; Herbst-Irmer, R.; Spek, A. L.; Schneider, T. R.; Sawaya, M. R. *Crystal Structure Refinement: A Crystallographer's Guide to SHELXL*; Oxford University Press, 2006.

(50) Torvisco, A.; Decker, K.; Uhlig, F.; Ruhlandt-Senge, K. Heavy Alkali Metal Amides: Role of Secondary Interactions in Metal Stabilization. *Inorg. Chem.* **2009**, *48*, 11459−11465.

(51) Allen, F. H. The Cambridge Structural Database: a quarter of a million crystal structures and rising. *Acta Crystallogr., Sect. B: Struct. Sci.* **2002**, *58*, 380−388.

DOI: 10.1021/acs.organomet.8b00258